

TOPOLOGICAL INSULATOR HETEROSTRUCTURES

by

Mahmoud Lababidi

A Dissertation

Submitted to the

Graduate Faculty

of

George Mason University

in Partial Fulfillment of

The Requirements for the Degree

of

Doctor of Philosophy

Physics

Committee:

---

Dr. Erhai Zhao,  
Dissertation Director

---

Dr. Dimitrios A. Papaconstantopoulos,  
Committee Member

---

Dr. Predrag Nikolic,  
Committee Member

---

Dr. Qiliang Li,  
Committee Member

---

Dr. Michael E. Summers,  
Director, School of Physics,  
Astronomy, and Computational Science

---

Dr. Timothy L. Born,  
Associate Dean for Student and Academic  
Affairs, College of Science

---

Dr. Vikas Chandhoke, Dean,  
College of Science

Date: \_\_\_\_\_

Summer Semester 2013  
George Mason University  
Fairfax, VA

## Topological Insulator Heterostructures

A dissertation submitted in partial fulfillment of the requirements for the degree of  
Doctor of Philosophy at George Mason University

By

Mahmoud Lababidi  
Bachelor of Science  
University of Florida, 2006

Director: Dr. Erhai Zhao, Professor  
 School of Physics, Astronomy and Computational Science

Summer Semester 2013  
George Mason University  
Fairfax, VA

Copyright © 2013 by Mahmoud Lababidi  
All Rights Reserved

## Dedication

To Angus Macgyver, who needed only a roll of duct tape, paperclip, and a Swiss Army knife to solve any problem.  
To my parents, Lina and Steve, for committing their lives for me, my future, and my success and happiness in life.

## Acknowledgments

First and foremost, I'd like to thank the most driven, understanding and supportive advisor anyone could ask for, Erhai Zhao. Not only have I learned more about physics than I could ever imagine, he has mentored me on being a good scientist, and a disciplined worker. I really could not have asked for a better advisor to lead me through this fascinating journey. I'd like to thank Dr. Papa for his incredible generosity from day one. He supported me throughout my PhD and without that support I would not have successfully completed the many projects and publications I have had. I consider Paul So to be more than just a graduate department advisor. You could add resident psychologist to his title and it would be wholly appropriate. Without his clear guidance on all top  including ones beyond physics and art, I would be a lost soul. I thank Mike Summers for his help as a department chair and helping me in times in need. He's supported me financially at times and has always had an open door for me and any graduate student to talk to him. Joe Weingartner would be considered the "House Dad" of the fraternity of the physics department. He has been a guiding light to me in many ways including physics and life. He is without a doubt one of the most important people the department has given tenure to for his kindness and empathy for anyone who walks into his office. I am very grateful to Indu Satija for her amazing creativity and beautiful ability to see physics like no one has. I give her full credit for the idea that spawned my most fascinating project of the driven quantum Hall system. I thank Predrag Nikolic, not only as helpful committee member but as great educator. He has always welcomed healthy discussion about a variety of topics that have helped me in my career numerous times. Qilian Li has been one of the most excited and appreciative members I could have on my committee. His enthusiasm in my work has been a heavy driver for a significant portion of my research. Ming Tian was the first person to take me under her wing as a student. She saw I had potential and ability to do physics and immediately gave me challenging problems to work on. She has been very supportive of my endeavours even if it meant changing groups. Without Kathleen Enos, Mari-Elaine Triolo, Geoff Elkins, Stephanie Monk, and Melissa Hayes I would be wrapped up in more paperwork than I could handle. They have made my this trip as smooth as possible and have been the best people to have around. Of course without Dan Thomas and Andrew Abdalian I'd be a headless chicken running around with regards to my IT issues. Phil Rubin was the person that urged me to apply to the program regardless of my physics background because he believed I'd do great. Somehow he was right. I later learned Phil was in a psychology PhD program when he switched to physics. That's serious inspiration. Gerald Cook was the first Professor I interacted with in my desire to start back in grad school. He was very enthusiastic for me to begin this journey. Stephen Gildea for inspiring me to go to graduate school by becoming a rocket scientist and kicking ass at it. Anish Mitra, my first friend in graduate school and roommate deserves much recognition for being the one person that was as interested in math and science as I was. Indrajit Das and Zrinka Greguric Ferencek are staples in my early career. I owe much to them for their stimulating discussions while we completed

course work together. Timofey Frolov is my favorite Russian physicist, metal guitarist, food snob I've ever known. He has been a great friend and colleague during our years at GMU before he ditched me for Berkeley.  Dirty himself, Greg Byrne, deserves more than a mention here for our antics during these years especially at the Arlington Office. Many thanks go to Devin Vega and our enjoyable and stimulating discussions in course work and research under Ming Tian. Quite importantly, I'd like to thank Lois Cohen, Edmund Lau, and Jean Wright for their influence during my formative high school years. I owe them more than just a line in this theses and without them I truly would not be here. The same goes for Anand Rangarajan and Eric Schwartz from my time at University of Florida, two professors who challenged me in innovative and creative ways. Not least, I'd like to thank SPACS, Office of Naval Research, Air Force Office of Scientific Research, National Science Foundation and National Institute of Standards and Technology for the funding they have provided me over these years.

## Table of Contents

	Page
List of Figures . . . . .	viii
List of Symbols . . . . .	xii
Abstract . . . . .	0
1 Introduction . . . . .	1
1.1 Topological Insulators . . . . .	1
1.2 Superconductivity . . . . .	7
1.2.1 Measurement . . . . .	7
1.2.2 BCS and Bogoliubov Theory . . . . .	9
1.3 Exotic systems with topological behavior . . . . .	13
1.3.1 $p_x + i p_y$ superconductors . . . . .	13
1.3.2 Fu-Kane Superconductor/Topological Insulator Model . . . . .	14
2 Metal to Topological Insulator Scattering . . . . .	17
2.1 Introduction . . . . .	18
2.2 Model Hamiltonian and Complex Band Structure . . . . .	20
2.3 Scattering Matrix from Wave-Function Matching . . . . .	23
2.4 Interface Spectrum and Scattering Matrix from Lattice Green Function . .	27
2.5 Discussions . . . . .	31
3 Superconducting Proximity Effect . . . . .	32
3.1 Introduction . . . . .	32
3.2 Model and Basic Equations . . . . .	35
3.3 Fourier Expansion . . . . .	42
3.4 The Order Parameter . . . . .	44
3.5 The Interface Mode and the Fu-Kane Model . . . . .	48
3.6 Triplet Pair Correlations . . . . .	50
3.7 Summary . . . . .	57
4 Josephson Junction on TI Surface . . . . .	60
4.1 Introduction . . . . .	60
4.2 Model . . . . .	61

4.3	Flat Bands in Spectrum . . . . .	66
4.4	Periodic $\pi$ Junction . . . . .	67
4.5	Summary . . . . .	68
	Bibliography . . . . .	72

## List of Figures

Figure	Page
1.1 (a) Energy spectrum of a trivial band insulator where two bands, conduction and valence are separated by an energy gap. (b) Energy spectrum of a quantum hall state. The gap now has one chiral edge state connecting the valence band to the conduction band. (c) Energy spectrum of a 2D TI (QSH). The gap now has one pair of chiral edge states connecting the valence band to the conduction band. One line is for the spin up state and the other is for the spin down state. This essentially mimics two copies of the quantum hall state for each spin. . . . .	3
1.2 Dirac cone dispersion. Energy as a function of momentum, $k_x$ and $k_y$ . . . . .	6
1.3 (left) Four probe measurement device. Probes 1 and 4 are used to flow a current across a sample while probes 2 and 3 measure the voltage drop across the sample where the current is flowing. (right) Resistance ( $\Omega$ ) vs Temperature (Kelvin) experiment on $\text{Cu}_{2.2}\text{Bi}_2\text{Se}_3$ from arXiv:1111.5805. The drop in resistance is a signature of superconductivity. . . . .	8
1.4 Energy spectrum for a BCS superconductor with a gap of $2\Delta_0$ and $\mu/\Delta_0 = 10$ . . . . .	12
1.5 Energy spectrum for a $p_x \pm ip_y$ superconductor with a chemical potential domain wall, ensuring linearly dispersing Majorana modes. . . . .	15
2.1 (a) Scattering geometry at a metal (M)-topological insulator (TI) interface. (b) Schematic band structure of the metal (modeled by $\hat{H}_M$ ) and topological insulator. . . . .	21
2.2 The complex band structure of topological insulator described by $\hat{H}_{TI}(\mathbf{k})$ for $k_y = 0$ , $k_x = 0.02$ (left) and $0.04$ (right). $E$ is measured in eV, and $k$ in $\text{\AA}^{-1}$ . Subgap states with complex $k_z$ represent evanescent waves. The topology of real lines [1] changes as $k_x$ is increased. . . . .	22

2.3	The magnitudes (upper panel) and the phases (lower panel) of the spin-flip amplitude $f$ and spin-conserving amplitude $g$ versus the incident angle $\theta$ . $E = 0.1\text{eV}$ , $E_F=0.28\text{eV}$ . $ g ^2 +  f ^2 = 1$ . $\text{Arg}(g)$ and $\text{Arg}(f)$ are shifted upward by $\pi$ for clarity. . . . .	26
2.4	The spectral function $N(E, k_x, k_y = 0)$ at the interface of metal and topological insulator. Left: good contact, $J = t_M$ , showing the continuum of metal induced gap states. Right: poor contact with low transparency, $J = 0.2t_M$ , showing well defined Dirac spectrum as on the TI surface. $t_M = 0.18\text{eV}$ , $\mu_M = -4t_M$ , $a$ is lattice spacing. . . . .	28
2.5	The spin-conserving reflection amplitude $ g $ and spin rotation angle $\alpha$ versus the incident angle $\theta$ for increasing contact transparency, $J/t_M = 0.25, 1, 1.5, 2$ (from left to right). $t_M = 0.18\text{eV}$ , $\mu_M = -4t_M$ , $E = 0.05\text{eV}$ , $k_y = 0$ . $ f ^2 = 1 -  g ^2$ . . . . .	29
3.1	Schematic (not to scale) band diagrams in a superconductor-topological insulator (S-TI) proximity structure. $E_f$ is the Fermi energy of the metal described by $H_M$ measured from the band crossing point. $\mu$ is the chemical potential of TI measured from the band gap center. The superconducting gap is much smaller than the band gap of TI. . . . .	37
3.2	The superconducting order parameter $\Delta(z)$ near an S-TI interface at $z = d = 0.95L$ . The superconductor occupies $0 < z < d$ , and topological insulator occupies $d < z < L$ . $L = 300 \text{ nm}$ , $\mu=0$ , the bulk gap $\Delta_0 = 0.6\text{meV}$ . . . . .	44
3.3	The order parameter $\Delta(z)$ near an S-TI interface at $z = d = 0.9L$ . $L = 160 \text{ nm}$ , $\mu=0$ , $\Delta_0 \sim 2.4\text{meV}$ . . . . .	46
3.4	The order parameter profile for two different chemical potentials of the topological insulator, $\mu = -0.1\text{eV}$ and $\mu = 0.2\text{eV}$ . $L = 160\text{nm}$ , $\Delta_0 \sim 5.2\text{meV}$ . . . . .	47
3.5	The lowest few energy levels $\epsilon_n(k_{  })$ . $\mu = 0$ , $L = 160\text{nm}$ , and the bulk superconducting gap $\Delta_0 \sim 5.2\text{meV}$ . A well-defined interface mode is clearly visible at sub-gap energies. Solid lines show a fit to the Fu-Kane model, with $\Delta_s = 1.8\text{meV}$ , $v_s = 2.7\text{eV}\text{\AA}$ , and $\mu_s = 7.5\text{meV}$ . . . . .	49
3.6	The dispersion of the lowest energy level for different $\mu$ (in eV). Other parameters are the same as in Fig. 3.5, $L = 160\text{nm}$ and $\Delta_0 \sim 5.2\text{meV}$ . Fu-Kane model well describes the lowest energy mode. As $\mu$ is increased, $\Delta_s$ and $v_s$ stay roughly the same, while $\mu_s$ scales linearly with $\mu$ . . . . .	51

3.7	The spectral function $N(k_{\parallel}, z, \omega)$ of the lowest energy level, $\omega = E_{min}$ , shown in Fig. 3.6. The interface is at $z = 0.9L$ , $L = 160\text{nm}$ . The spectral function oscillates rapidly with $z$ , so only its envelope is plotted. . . . .	52
3.8	The local density of states $N(E, z)$ at $z = 0.8d$ and $z = 0.85d$ (the interface is at $z = 0.9d$ ). $\mu = 0$ , $L = 160\text{nm}$ , and $\Delta_0 \sim 5.2\text{meV}$ . The subgap states are due to the interface mode. A level broadening $\sim 0.01\Delta_0$ is used. . . . .	53
3.9	The lowest energy level of an S-TI structure with $L = 160\text{nm}$ , $d = 0.9L$ , $\Delta_0 = 2.4\text{meV}$ . $\mu$ is the chemical potential of the TI and measured in eV. . . . .	54
3.10	The imaginary part of triplet pair correlation function $F_{\uparrow\uparrow}(k_{\parallel}, z)$ . The S-TI interface is at $d = 0.9L$ . $\mu = 0$ , $L = 160\text{nm}$ , $\Delta_0 = 5.2\text{meV}$ . . . . .	56
3.11	The imaginary part of $F_{\uparrow\uparrow}(k_{\parallel}, z)$ . $\mu = 0$ , $L = 300\text{nm}$ , $d = 0.95L$ , $\Delta_0 = 0.6\text{meV}$ . As comparison, the data points show the singlet pair correlation function $F_{\uparrow\downarrow}(k_{\parallel}, z = 0.9L)/3$ . . . . .	58
4.1	(color online) a) Schematic of a Josephson junction on the surface of a topological insulator (TI). The two superconducting leads (S) have a phase difference $\pi$ . $\Delta$ is the superconducting gap, and $w$ is the junction width (not to scale). b) Specular Andreev reflection in the regime $E > \mu$ . c) Retro-reflection for $E < \mu$ . d) Dark lines show the $(k_y, \mu)$ values for the zero energy Andreev bound states for $w = 10\hbar v_F/\Delta$ and $L \rightarrow \infty$ . $k_y$ is in unit of $\Delta/\hbar v_F$ . . . . .	62
4.2	(color online) The local spectral function $A_{\uparrow}(E, k_y, x)$ (upper panel) and local density of states $N(E, x)$ (lower panel, red solid line) at the center of the junction, $x = 0.5L$ . One sees “flat” Andreev bound states near zero energy for $-k_F < k_y < k_F$ , and correspondingly a pronounced peak at zero energy in the LDOS in the lower panel. The lower panel also shows different LDOS away from the center, for $x$ from $0.52L$ to $0.58L$ . . . . .	65
4.3	(color online) Upper panel: Schematic of the periodic proximity structure with $\Delta(x) = \Delta \sin(\pi x/a)$ . The wave function $ u(x) $ for the zero energy states are peaked at the domain wall boundaries, $x = ma$ . Lower panel: Energy spectrum for $a = 24\hbar v_F/\Delta$ and $\mu = 4\Delta$ is flat at zero energy, which has fine structures upon closer inspection. . . . .	70

4.4 Fine structures in the energy spectrum of the periodic proximity structure with fixed  $a = 12\hbar v_F/\Delta$  and increasing  $\mu$ . The linearly dispersing Majorana spectrum at  $\mu = 0$  splits and develops curvature to eventually become nearly flat within  $(-k_F, k_F)$ . The number of zero energy crossings increases with  $\mu$ . 71

## List of Symbols

$v_F$	Fermi velocity of Dirac electrons
$\vec{k}$	momentum vector
$k_i$	momentum in the $i$ -th direction
$\mathcal{E}_F$	Fermi energy
$A(x, k, \epsilon)$	spin( $\sigma$ ), momentum and position resolved density of (energy) states
$N(x, \epsilon)$	spin( $\sigma$ ) and position resolved density of (energy) states
$\mu$	chemical potential, sometimes as Fermi energy ( $\mathcal{E}_F$ )
$\mathcal{H}$	Hamiltonian
$\psi(x)$	wave function of particle
$u_\sigma$ ( $v_\sigma$ )	Bogoliubov-de Gennes quasi-particle (hole) wave function
$k_B$	Boltzmann's constant

## **Abstract**

TOPOLOGICAL INSULATOR HETEROSTRUCTURES

Mahmoud Lababidi, PhD

George Mason University, 2013

Dissertation Director: Dr. Erhai Zhao



abstract here.

# Chapter 1: Introduction

This thesis presents a systematic study of the interaction and interplay between a new class of materials named Topological Insulators (TIs) and superconductors. It is broken down into five chapters. The first chapter contains an introduction to TIs and superconductors. In addition, it describes additional material that is built upon in the results of the thesis. These include the topological surface states of a TI, the spin texture of the TI surface, phenomenological description of a superconductor coupled to a TI, exotic superconductors, and a Josephson junction structure on a TI surface. These topics are accepted in the community and not meant to be presented as new results. The second chapter presents a study of metal on TI (M-TI) electron scattering and interaction. This chapter provides information to understanding the effect of spin-orbit interactions on arbitrary spin-polarized electrons. The third chapter is the microscopic study of superconductors with TIs. A heterostructure of a superconductor with a TI is studied in the context of superconductivity to understand the effect of a topological insulator. The fourth chapter explores a proposed Josephson junction structure on a TI surface and delves into new effects in regimes not looked at before. Each chapter beyond the first represents a published work.

## 1.1 Topological Insulators

The field of condensed matter physics has a history of understanding phases of matter that have been condensed where the early focus was on solids and liquids. The field has transitioned into studying a variety of novel phases that are very rich and complex in physical phenomena. As a result of the exploration of many novel phases, the concept of order arose, allowing, not only the ability to categorize these phases by recognizing the type of order the system had but the order and symmetry actually described the physical system

and allowed a deeper understanding. This idea is clearly seen in the phase transition of liquid atoms with rotational and translational symmetry into a crystal with discrete symmetries (e.g. translational, discrete rotational, inversion). An extension to this would be a solid transitioning into a magnet, thus breaking inversion symmetry. While this study of symmetry breaking is at the heart of condensed matter, it is not the full story.

In 1980 Klaus von Klitzing performed an experiment measuring the Hall conductance of a special semiconductor heterostructure [2]. What he found in the experiment was that the measured conductance came in exact quantized fundamental units of

$$\sigma = \nu \frac{e^2}{h}, \quad (1.1)$$

where  $\nu$  is an integer value. The significance of this result, was not only in the quantized nature of the Hall conductance, but something a bit deeper. This quantum Hall effect was special because this result could not be predicted through the usual symmetry breaking language. In the heterostructure used in the experiment, the internal “bulk” of the system is effectively a two dimensional electron gas exposed to a strong magnetic field. The strong magnetic field puts the electrons in a cyclotron orbit and forces the electrons into discrete energy levels, Landau levels. This effect is the same as a harmonic oscillator where an electron is in a spatially quadratic electric potential well ( $V(x) \propto x^2$ ). These separated energy levels allows for the system to be an insulator when the Fermi energy is placed within the gap between two separate energy levels. While this system is in an insulating state, the special result of von Klitzing’s experiment is that the edge is still a host to electronic states that propagate in a chiral manner. This discrepancy between the ability to describe bulk of the material and its edge is the issue at hand.

The quantum Hall effect (QHE) is actually a topological phase, meaning it has topological order. Systems with topological order have long-range entanglement and a ground state degeneracy that cannot be lifted by any local perturbation. These systems are protected from being deformed into a phase with different topology in the same way a donut (torus)

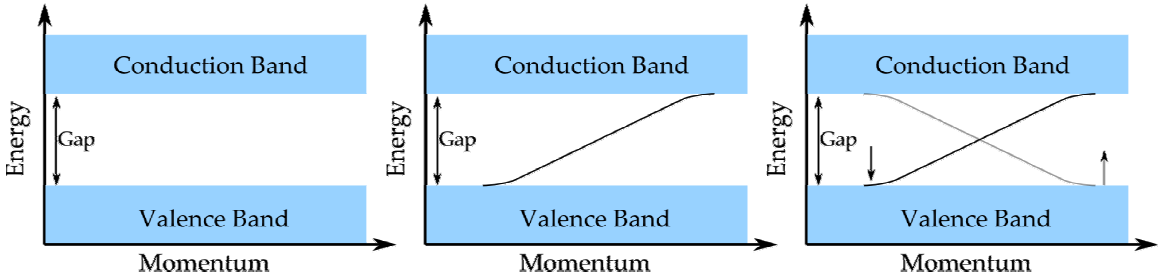


Figure 1.1: (a) Energy spectrum of a trivial band insulator where two bands, conduction and valence are separated by an energy gap. (b) Energy spectrum of a quantum hall state. The gap now has one chiral edge state connecting the valence band to the conduction band. (c) Energy spectrum of a 2D TI (QSH). The gap now has one pair of chiral edge states connecting the valence band to the conduction band. One line is for the spin up state and the other is for the spin down state. This essentially mimics two copies of the quantum hall state for each spin.

is protected from being deformed into a sphere. The only time such a change is possible is through a phase transition where the gap in the energy spectrum closes in a critical fashion. Many discussions on topological order can be found in many literature and any continued discussion about topological order in farther depth would not be appropriate, for this thesis does not represent any study of topological order in this form.

We, instead, will continue by using the QHE as a lead-in for the topological insulator. Though the topological insulator is a slight misnomer because of the lack of topological order (i.e. long-range entanglement), we will shortly see where the topology plays a role in it. By taking the QHE, we can extend it in the following way. The QHE is a gapped system with chiral edge states that depend on the applied magnetic field (see Fig. The chirality of the edge states depend on the direction of the magnetic field, i.e. positive (negative) chiral motion of the electrons for positive (negative) in-plane magnetic field. If a system were to have both positive and negative magnetic fields simultaneously for two different species of electrons, we would see the electrons follow the two chiral motions simultaneously depending

on their species. The two different species of electrons are, of course, spin-up and spin-down electrons which couple to the two magnetic fields. This system is the quantum spin hall effect. This system, first introduced by Kane and Mele, was proposed to exist in graphene [3]. Shortly afterwards Bernevig, Hughes, and Zhang proposed an experimental setup to host the QSH effect [4]. Their proposal, which was verified successfully in an experiment by Koenig [5], exploited the spin-orbit coupling and band inversion in a HgTe CdTe HgTe heterostructure to create simultaneous opposite chirality edge states. The QSH insulator, is a 2D topological insulator. An effective Hamiltonian for the edge state can be written as

$$H = \hbar v_F \sigma_x k_y, \quad (1.2)$$

where the basis is for spin up and spin down and the resulting eigen energies are  $E = \pm \hbar v_F k_y$ .  $\hbar v_F$  is the Fermi velocity slope. This is a massless Dirac Hamiltonian and the spectrum forms a Dirac crossing.

The existence of a surface state can be seen in the following manner. If a topological insulator has a parameter that can be tuned to transition the TI from non-trivial to trivial, the gap of the insulator closes. When a TI is interfaced with a trivial insulator, such as the vacuum, the parameter effectively closes the gap spatially at the transition point between the insulators. This is the closed gap (gapless) surface state.

In principle, by stacking sheets of the 2D TIs and forming a 3D structure, this would be a “weak” topological insulator. The other extension of the TI from 2D to 3D is a “strong” topological insulator. Here, there is also an insulating 3D bulk and the 2d surfaces interface the vacuum and these surface states are similar to the edge state of the 2D TI in their linear dispersing behavior, but in contrast they allow momentum to be in any in-plane direction,  $\vec{k} = (k \cos(\theta), k \sin(\theta))$ . The effective low-energy Hamiltonian for these surface states is

$$H = \hbar v_F (\sigma_x k_y - \sigma_y k_x). \quad (1.3)$$

The energies and their respective eigenvectors

$$E = \pm \hbar v_F |\vec{k}| \quad |\psi_{\mathbf{k}}\rangle = \pm ie^{-i\theta} |\uparrow\rangle + |\downarrow\rangle \quad (1.4)$$

where  $|\vec{k}| = \sqrt{k_x^2 + k_y^2}$  and  $|\uparrow\rangle (|\downarrow\rangle)$  is the spin up (down) state.

We plot the energy dispersion as a function of  $k_x$  and  $k_y$  to find a Dirac cone as the shape of the surface in Fig. 1.2. Any cut taken for some value of  $E \neq 0$  produces a circle of states. The eigenstates are always equal superpositions of spin up and down, meaning the spinor is pointing in the x-y plane. The exact direction is dictated by the phase ( $ie^{i\theta}$ ), or the spin is pointing  $\pi/2$  angle difference from the momentum direction angle,  $\theta$ , due to the extra  $i$ .

If we look closely at the spin-momentum relationship we see that it is not possible to have arbitrary spin and momentum in an electron on the TI surface. Every direction of momentum belongs to one direction of spin and vice versa. This can be seen as a broken symmetry of the surface electrons where they no longer have arbitrary spin and momentum. This surface is very different from a normal metal where spin is arbitrary for any momentum and also different from a ferromagnetic where the spin on an electron is fixed but can have arbitrary momentum. This coupling along with the relativistic energy dispersion is unique and provides a playground for many exotic properties. These include Majorana fermions[6, 7, 8, 9], barrier transmission [10], spin-currents [11, 12], Aharonov-Bohm oscillations [13], Shubnikov-de Haas oscillations [14], Landau level quantization [15], massive relativistic Dirac fermions [16, 17] and exciton condensation [18].

This concludes the basic description of the TI. We showed how a 2D TI was produced using two copies of a QH system with opposite simultaneous magnetic fields. We then extended the idea of a 2D TI to 3D “weak” and “strong” TIs. We then examined the surface states to understand the relationship between the spin and momentum as well as potential implications and applications.

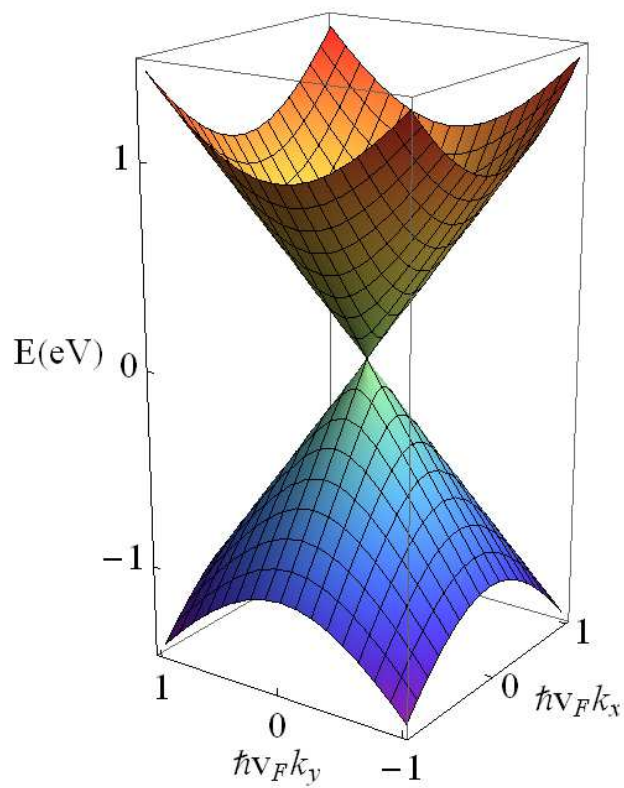


Figure 1.2: Dirac cone dispersion. Energy as a function of momentum,  $k_x$  and  $k_y$ .

## 1.2 Superconductivity

### 1.2.1 Measurement

The discovery of superconductivity by Heike Kamerlingh Onnes is usually the first item that's discussed when the topic of superconductivity is brought up. In the discovery, Onnes found that the resistance of mercury drops to zero, a signature of perfect conduction. The immediate question that rang in my head, if using a typical voltmeter, as used in physics labs, and Ohm's law,  $V = IR$ , how can resistance or voltage be measured if they should both be zero? The result is by using a four point probe. As seen in the diagram in Fig. 1.3, the probe has four point of contact on the material. Two of the connections (1,4) have a constant, controllable current flowing through them. The other two connections (2,3), then probe the sample and measure the voltage drop. The voltage measurement device has a high impedance to minimize any flow from the sample to flow into it. The resulting voltage drop,  $V$ , and driving current,  $I$ , then give the resistance,  $R = V/I$ , which along with temperature results in a temperature dependent resistance. An example measurement of  $\text{Cu}_2\text{Bi}_2\text{Se}_3$ , a new superconducting material is shown in Fig. 1.3. The plot shows a clear resistance drop at 3.5 Kelvin, the signature of superconductivity.

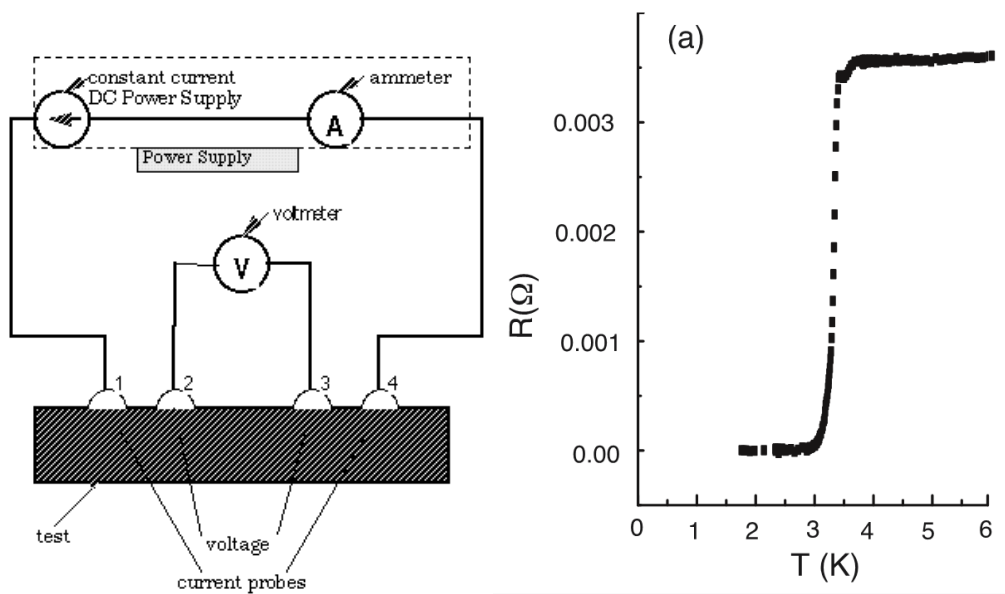


Figure 1.3: (left) Four probe measurement device. Probes 1 and 4 are used to flow a current across a sample while probes 2 and 3 measure the voltage drop across the sample where the current is flowing. (right) Resistance ( $\Omega$ ) vs Temperature (Kelvin) experiment on  $\text{Cu}_{2}\text{Bi}_2\text{Se}_3$  from arXiv:1111.5805. The drop in resistance is a signature of superconductivity.

### 1.2.2 BCS and Bogoliubov Theory

Now that the question of how to find and measure superconductivity is out of the way, we can look at the theory that Bardeen, Cooper, and Schreiffer (BCS) came up to explain the mechanism behind superconductivity. We start with the Hamiltonian that represents a free electron system with two-body electron interactions,

$$H = \sum_{\mathbf{k},\sigma} (\epsilon_{\mathbf{k}} - \mu) c_{\mathbf{k}\sigma}^\dagger c_{\mathbf{k}\sigma} + \sum_{\mathbf{k},\mathbf{l}} V_{\mathbf{k}\mathbf{l}} c_{\mathbf{k}\uparrow}^\dagger c_{-\mathbf{k}\downarrow}^\dagger c_{-\mathbf{l}\uparrow} c_{\mathbf{l}\downarrow} \quad (1.5)$$

where  $c_{\mathbf{k}\sigma}^\dagger$  ( $c_{\mathbf{k}\sigma}$ ) is the electron creation (annihilation) operator, the summations are over spin ( $\sigma$ ) and momentum ( $\mathbf{k}, \mathbf{l}$ ),  $\epsilon_{\mathbf{k}}$  is the free electron energy,  $V_{\mathbf{k}\mathbf{l}}$  is the electron-electron interaction potential. The commutation relations for the fermion creation and annihilation operators are

$$\{c_{\mathbf{k}\sigma}^\dagger, c_{\mathbf{k}'\sigma'}\}_+ = \delta(\mathbf{k} - \mathbf{k}') \delta_{\sigma\sigma'} \quad (1.6)$$

$$\{c_{\mathbf{k}\sigma}^\dagger, c_{\mathbf{k}'\sigma'}^\dagger\}_+ = \{c_{\mathbf{k}\sigma}, c_{\mathbf{k}'\sigma'}\}_+ = 0. \quad (1.7)$$

In usual electron systems, the interaction scattering potential,  $V_{\mathbf{k}\mathbf{k}'}$ , usually positive, represents repulsive interactions. But as the temperature is lowered, what BCS explained was that the repulsive interaction was no longer the dominant interaction. Instead, what occurs at zero temperature is the following. As an electron passes through a lattice of low-mobility nuclei, they actually cause the nuclei to shift causing a phonon interaction with electron. This phonon interaction is enough to effectively attract,  $V_{\mathbf{k}\mathbf{k}'} < 0$ , two electrons with opposite momenta( $\mathbf{k}, -\mathbf{k}$ ). From the Pauli exclusion principle, we seek a bound pair of electrons with zero momentum, antisymmetric, spin-less properties, known as a Cooper pair. This pair of electrons forms a boson with superflow that is responsible for the lack of resistance. The electrons near the Fermi energy are most susceptible to pairing, usually when they are within some Debye energy cutoff,  $\hbar\omega_D$ . When the electrons pair, they form a condensate of the bosons. One way to describe these bosons is through a condensate

wave function,  $\Delta(\mathbf{x})$ , or  $\Delta_{\mathbf{k}}$ . This function is found by a mean field approach to the pairing potential,  $V_{\mathbf{kk}'}$ , through the gap equation

$$\Delta_{\mathbf{k}} = \sum_{\mathbf{k}'} c_{-\mathbf{k}\uparrow} c_{\mathbf{k}\downarrow} \quad (1.8)$$

reducing the Hamiltonian down to

$$H = \sum_{\mathbf{k},\sigma} (\epsilon_{\mathbf{k}} - \mu) c_{\mathbf{k}\sigma}^\dagger c_{\mathbf{k}\sigma} + \sum_{\mathbf{k}} \Delta_{\mathbf{k}} c_{\mathbf{k}\uparrow}^\dagger c_{-\mathbf{k}\downarrow}^\dagger. \quad (1.9)$$

To diagonalize this Hamiltonian we change the basis, where rather than restricting ourselves to operators of electrons, we use the Bogoliubov-de Gennes (BdG) transformation to convert the operators on elementary quasiparticle excitations of particles and holes. This is done through

$$c_{\mathbf{k}\sigma} = \sum_n u_{n\mathbf{k}\sigma} \gamma_{n\mathbf{k}} + v_{n\mathbf{k}\sigma}^* \gamma_{n\mathbf{k}}^\dagger, \quad c_{\mathbf{k}\sigma}^\dagger = \sum_n u_{n\mathbf{k}\sigma}^* \gamma_{n\mathbf{k}}^\dagger + v_{n\mathbf{k}\sigma} \gamma_{n\mathbf{k}} \quad (1.10)$$

where the BdG operators fulfill the anti-commutation relations,

$$\{\gamma_{\mathbf{k}\sigma}^\dagger, \gamma_{\mathbf{k}'\sigma'}\} = \delta_{\mathbf{k}\mathbf{k}'} \delta_{\sigma\sigma'} \quad \{\gamma_{\mathbf{k}\sigma}, \gamma_{\mathbf{k}'\sigma'}\} = \{\gamma_{\mathbf{k}\sigma}^\dagger, \gamma_{\mathbf{k}'\sigma'}^\dagger\} = 0 \quad (1.11)$$

and allow us to diagonalize the Hamiltonian as

$$H = E_0 + \sum_{\mathbf{k},\sigma} E_{\mathbf{k}} \gamma_{\mathbf{k}\sigma}^\dagger \gamma_{\mathbf{k}\sigma}. \quad (1.12)$$

The quasiparticle (quasi-hole) wave function is  $u_{\mathbf{k}\sigma}$  ( $v_{\mathbf{k}\sigma}$ ). Each electron creation/annihilation operator is a superposition of a quasiparticle creation and annihilation operator. The inverse

of this transformation,

$$\gamma_{\mathbf{k}\sigma} = \sum_n u_{n\mathbf{k}\sigma} c_{n\mathbf{k}} - v_{n\mathbf{k}\sigma}^* c_{n\mathbf{k}}^\dagger, \quad \gamma_{\mathbf{k}\sigma}^\dagger = \sum_n u_{n\mathbf{k}\sigma}^* c_{n\mathbf{k}}^\dagger - v_{n\mathbf{k}\sigma} c_{n\mathbf{k}} \quad (1.13)$$

leads to each quasiparticle operator being a superposition of one electron creation operator and one hole creation operator, thus the sum net charge is zero for each BdG creation/annihilation operator. This physical interpretation allow us to see that there is more to the story than just electrons and holes, but elementary quasiparticle excitations of pairs of holes and electrons.

The form of the BdG Hamiltonian is

$$H_B = \begin{pmatrix} \epsilon_{\mathbf{k}} - \mu & -\Delta_{\mathbf{k}} i\sigma_y \\ \Delta_{\mathbf{k}}^* i\sigma_y & \mu - \epsilon_{\mathbf{k}} \end{pmatrix}, \quad (1.14)$$

in the basis of

$$\psi = (u_{\mathbf{k}\uparrow}, u_{\mathbf{k}\downarrow}, v_{\mathbf{k}\uparrow}, v_{\mathbf{k}\downarrow})^T. \quad (1.15)$$

The  $\Delta_{\mathbf{k}}$  can come in a variety of forms, strictly depending on the pairing symmetry of the superconductor. In the BCS case, we focus on  $\Delta_{\mathbf{k}} = \Delta_0$ , a constant value, representing s-wave orbital pairing. This allows us to find the eigen values of the system,

$$E_{\mathbf{k}} = \pm \sqrt{(\epsilon_{\mathbf{k}} - \mu)^2 + |\Delta|^2}. \quad (1.16)$$

where the spectrum can be seen in the Fig. 1.4. There is now a finite gap of size  $2\Delta_0$  seen centered about 0. The gap is a result of the pairing that occurs in the superconductor. These paired states form the condensate,  $\Delta$ , and no low energy excitations can exist within the energy gap in the spectrum. In order for an excitation to move a paired state out of the condensate, you would need  $\Delta_0$  energy to break the pair.

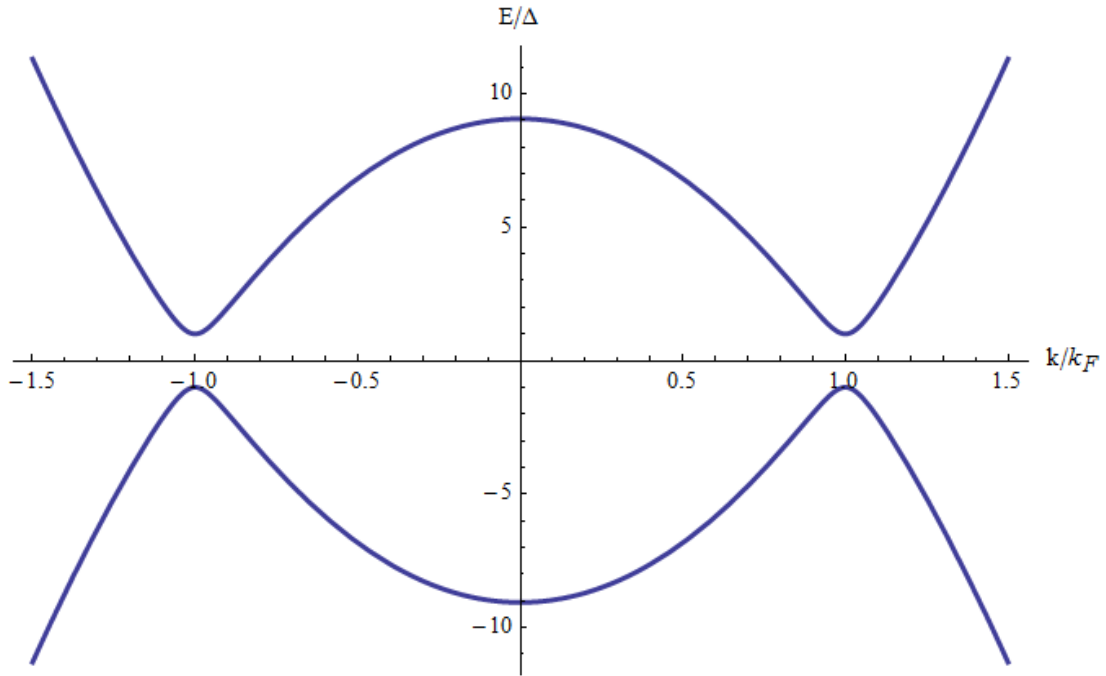


Figure 1.4: Energy spectrum for a BCS superconductor with a gap of  $2\Delta_0$  and  $\mu/\Delta_0 = 10$ .

This concludes the section on superconductivity. Here we described a basic idea on how to measure a superconductor using a four-probe measurement, we describe the BCS theory on superconductivity to describe the mechanism behind the Cooper pairing, and we diagonalized the BCS Hamiltonian using a mean field approximation and a Bogoliubov-de Gennes Transformation, which allowed us to investigate the energy spectrum. These should be the building blocks for understanding the discussion on superconductivity in this thesis.

## 1.3 Exotic systems with topological behavior

This section presents the motivation for understanding a couple of condensed matter systems that have exotic properties related to topological insulators. These are  $p_x+ip_y$  superconductors and topological insulator-superconductor heterostructures that host Majorana Fermions. These systems have implications in understanding the role of topology in superconducting systems as well as the possibility of topological quantum computation through the Majorana fermion. The chapters beyond the introduction provide deeper study of these systems beyond phenomenology.

### 1.3.1 $p_x+ip_y$ superconductors

One model of a superconductor that has exotic topological behavior is the  $p_x+ip_y$  superconductor. The symmetry of this paired spin-triplet state is of the form  $\Delta_k = \Delta_0(k_x + ik_y)$ . If we apply this form of the pairing into (1.14), we can diagonalize this Hamiltonian and find eigen values of the form

$$E_{\mathbf{k}} = \pm \sqrt{(\epsilon_{\mathbf{k}} - \mu)^2 + (\Delta_0|\mathbf{k}|)^2}. \quad (1.17)$$

This differs from the conventional s-wave eigen energies because the gap term now depends on  $\mathbf{k}$ . For values of  $\mu \gg 0$ , this doesn't effect the spectrum by any more then a negligible change. The noticeable difference, as described the Read and Green, is when the Fermi energy is reduced to a small value so that  $(\epsilon_{\mathbf{k}} - \mu) \rightarrow -\mu$ . The spectrum then evolves into a spectrum for a relativistic Dirac fermion with mass  $\mu$  and speed of light  $\Delta_0$ . We also write the BdG equations in the form of

$$Eu = -\mu u + \Delta^* i(\partial_x + i\partial_y)v \quad (1.18)$$

$$Ev = \mu v + \Delta i(\partial_x - i\partial_y)u. \quad (1.19)$$

This is a form of the Dirac equation, and the BdG equations allow for  $u = v^*$ , where at each  $\mathbf{k}$  there is only one excitation mode. This shows that the particles,  $u$ , are their own anti-particles,  $v$ . When a Dirac fermion has this property, it is a Majorana Fermion. In this topological system we can take the mass term to vary spatially through a domain wall ( $\mu(x) \propto \text{sign}(x - x_0)$ ), by tuning the Fermi energy spatially. The requirement for the domain wall is due to the parameter ( $x$ ) dependent transition from a trivial state superconductor,  $\mu < 0$  to a non trivial topological superconductor,  $\mu > 0$ . One simple model to do this is by  $\mu(x) = \mu \sin(2\pi x/L)$ . We find a spectrum with linear modes in Fig. 1.5. The linear Majorana modes are found to have chiral propagation and reside at the centers of the domain walls. Another way to host a Majorana in a p-wave superconductor is by imposing a vortex through a magnetic field, where at the core and edge of the vortex reside the Majorana fermions.

### 1.3.2 Fu-Kane Superconductor/Topological Insulator Model

Here we present a model by Fu and Kane to simulate the effect of a superconductor in close proximity to the surface of a TI. The TI has the Hamiltonian in the form of  $H = v_F(\sigma_x k_y - \sigma_y k_x) - \mu$ , where  $k_i$  are the momenta,  $\sigma_i$  are the Pauli spin matrices, and  $v_F$  is the Fermi velocity. If an s wave superconductor is brought to the surface of the TI, Fu-Kane argued that the surface Hamiltonian will stay consistent, but will now have pairing to reckon with.

This interplay between a TI and S presents many possibilities of various physical effects. This system can be seen as a host for a spin-less  $p_x \pm i p_y$  superconductor. Also, under certain conditions where there is a domain wall through the superconductor order parameter,  $\Delta$  or a magnetic domain wall, it is expected to find a Majorana mode.

Fu-Kane argued that the form of the pairing term is also consistent from the S side to

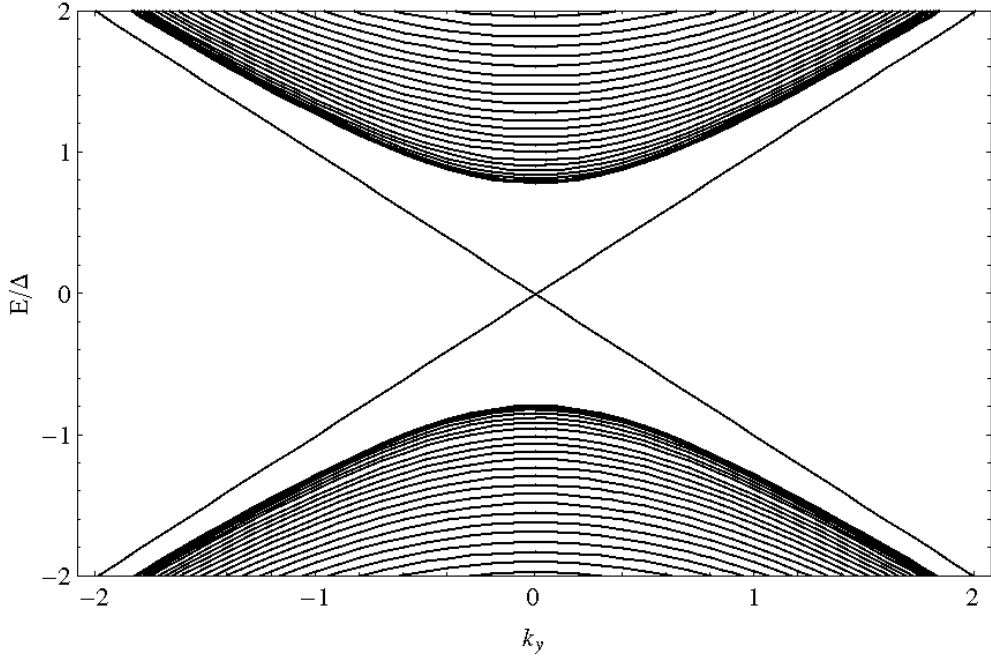


Figure 1.5: Energy spectrum for a  $p_x \pm ip_y$  superconductor with a chemical potential domain wall, ensuring linearly dispersing Majorana modes.

the TI side producing the following BdG Hamiltonian

$$\mathcal{H}(\mathbf{k}) = \begin{pmatrix} H(\mathbf{k}) & i\sigma_y\Delta \\ -i\sigma_y\Delta^* & -H^*(-\mathbf{k}) \end{pmatrix} = v_F(\sigma_x k_y - \tau_z \sigma_y k_x) - \tau_z \mu + \tau_y \sigma_y \Delta. \quad (1.20)$$

The spectrum for this system is

$$E = \sqrt{|\Delta|^2 + (v_F |\mathbf{k}| \pm \mu)^2}. \quad (1.21)$$

This system is very analogous to the p-wave superconductor. If we take the limit  $\mu u \rightarrow 0$

this dispersion is also relativistic where the mass term is  $\Delta$  and the speed of light is  $v_F$ . The  $p_x \pm ip_y$  term is responsible for the  $\mathbf{k}$ -dependent gap and the resulting Majorana mode. In the superconductor-TI heterostructure, this term is also, as we shall see soon, responsible for producing Majorana modes. Since, this is a topological system, the mass term is parameter that can be tuned to close the gap at one (or an odd number of points) in the spectrum. The mass term in the S-TI system is the gap parameter,  $\Delta$ . If we allow  $\Delta$  to flip sign spatially from a positive value,  $|\Delta_0|$ , to a negative value,  $-|\Delta_0|$ , through  $\Delta(x) = \Delta_0 \tanh(x/L)$ , we find a Majorana mode localized at the point where  $\Delta(x) = 0$  ( $x = 0$ ) with a linear dispersion that resembles the spectrum of the p-wave superconductor edge-state in Fig. 1.5. One difference is the TI version is four-fold degenerate (particle/hole and spin) at  $E = 0$  while the p-wave is two-fold degenerate (particle/hole). Both systems' linear dispersing states are localized at the domain wall,  $x = 0$ . This domain wall can be seen as a Majorana wire in the y-direction.

We've now shown some superconductors with exotic properties. We looked at the p-wave superconductor and how it can be tuned to host Majorana modes along with it's relativistic Dirac-like energy dispersion. We also looked at the Fu-Kane TI-S heterostructure and also found it can be tuned to host Majorana modes. These systems are very analogous to each other and show the potential of the potential exotic properties through the TI. The Fu-Kane system are the starting point for latter two thirds of the thesis where we study TI-S structures in greater detail.

## Chapter 2: Metal to Topological Insulator Scattering

As described in Chapter 1, the topological insulator (TI) has a  surface where the spin and momentum of an electron are coupled such that the direction of the spin is equal to the direction of the momentum plus  $\pi/2$ . That is to say, the electron's wave function,  $|\psi_{\mathbf{k}}\rangle$ , is presented as

$$|\psi_{\mathbf{k}}\rangle = \pm ie^{-i\theta} |\uparrow\rangle + |\downarrow\rangle \quad (2.1)$$

where  $\theta = \arctan(k_y/k_x)$  and  $|\uparrow\rangle(|\downarrow\rangle)$  is the spin up (down) state. It's clear that the phase  $ie^{-i\theta}$  dictates the direction of the spin in the  $x - y$  plane. This special surface is the motivation for the following chapter.

Since we understand the spin-momentum behavior of the electrons that reside on the surface of the TI, a natural extension would be to understanding electrons that scatter off the surface of a TI. Any incoming electron has an interaction with the spin-orbit coupling of the TI. This interaction dictates the resulting spin of the reflected electron.

We find that for a certain critical angle, the electron's spin will always flip, regardless of its state before reflection (i.e.  $\alpha|\uparrow\rangle + \beta|\downarrow\rangle \rightarrow \alpha|\downarrow\rangle + \beta|\uparrow\rangle$ ). This is very different from reflection from a ferromagnetic insulator, where incoming electrons polarize to have their spin eventually point in the direction of magnetization of the ferromagnet. This clear difference is unique and allows for an ability to control electrons arbitrarily and perform NOT-gate like operations in binary logic devices, (i.e.  $\text{TRUE} \rightarrow \text{FALSE}$  and  $\text{FALSE} \rightarrow \text{TRUE}$ ).

To understand this spin dependent interaction we propose the problem as a metal-TI setup. The left half, spatially, is a metal and the right half is the TI. An incoming electron comes from the metal side and  to the TI. Since the TI is an insulator, incoming electrons do not propagate through but rather reflect back to the metal side. We calculate the spin dependent reflection coefficients of the reflected electron. This spin-resolved reflection has

implications in using TIs for spintronics because of the ability to invert the spin direction, hence negate the information stored on there.

In addition to the scattering approach, we seek to understand in the combined effect that the metal and TI have when they are in contact with each other in a different perspective. We do this by using a lattice Green's function method to find the resulting spatially resolved energy spectrum and to calculate the scattering coefficients, also. We find that the local spectrum has two limits depending on the strength of the tunneling between the metal and TI. For good tunneling we find that the metal has a stronger influence on the on spectrum near the surface where for weak contacts the Dirac cone is clear and well-defined.

Lastly, we discuss the complex energy spectrum of the TI ( $E(k_{\text{Real}}, k_{\text{Imag}})$ ,  $k_z \rightarrow k_{\text{Real}} + ik_{\text{Imag}}$ ). It gives us insight into understanding the behavior of the surface localized wave function of the Dirac electrons.

## 2.1 Introduction

Recently discovered three dimensional topological band insulators [19, 20, 21], such as  $\text{Bi}_{1-x}\text{Sb}_x$  [22] and  $\text{Bi}_2\text{Se}_3$  [23, 24, 25], are spin-orbit coupled crystal solids with a bulk gap but protected gapless surface states. The low energy excitations at the surface are helical Dirac fermions, i.e., their spin and momentum are entangled (locked) [26]. The charge and spin transport on the surface of a topological insulator are intrinsically coupled [27]. This makes these materials a promising new platform for spintronics. In addition, heterostructures involving topological insulator, superconductor, and/or ferromagnet have been predicted to show a remarkable array of spectral and transport properties (for review see Ref. [28, 29, 30]).

Electronic or spintronic devices based on topological insulators will almost inevitably involve metal as measurement probes or functioning components [31]. This motivates us to study the local spectrum near the interface between a metal (M) and a topological insulator (TI). For a metal-ordinary semiconductor junction with good contact, it is well known that

## Chapter 3: Superconducting Proximity Effect

In the first chapter we described the topological insulator and it's novel features. We also described the exotic  $p-$  wave superconductor and along with the topological insulator in proximity to an  $s-$ wave superconductor. We showed that these systems are topological in the sense that there exist bound states that exist with gap-less energy spectrum localized near certain boundaries. These edge states have linear Dirac dispersions

In this chapter we focus on the superconductor-topological insulator heterostructure. This structure is predicted by Fu and Kane to be a host to a Majorana fermion under certain conditions. Our focus is not  the phenomenological properties of the Majorana regime, but rather to understand the behavior of the system under certain regimes in a realistic fashion. We set up the Bogoliubov-de Gennes model for a TI and a superconductor to calculate the eigensystem in a recursive, self-consistent manner. The eigen energies and wave functions provide the framework we need to calculate several quantitative properties. These include order parameter,  $\Delta(z)$ , spatially resolved spectral function,  $A(z, k, \epsilon)$ , local density of states,  $N(z, \epsilon)$ . In addition we also find singlet ( $F_{\uparrow\downarrow}(k, z)$ ) and triplet ( $F_{\uparrow\uparrow}(k, z)$   $F_{\downarrow\downarrow}(k, z)$ ) correlations. We show that the energy spectrum does indeed host sub-gap states as predicted by Fu-Kane which are renormalized. We also find triplet correlations, exhibiting  $p_x + ip_y$  behavior, consistent with previous studies of a similar system.

### 3.1 Introduction

Fu and Kane showed that at the interface between a three-dimensional topological band insulator (TI) and an  $s$ -wave superconductor (S) forms a remarkable two-dimensional non-Abelian superconductor [47]. It hosts Majorana zero modes at vortex cores, as in a  $p_x + ip_y$  superconductor [48], but respects time-reversal symmetry. As argued in Ref. [47], the

## Chapter 4: Josephson Junction on TI Surface

So far, we have found that near the interface between the topological insulator and a superconductor is a host to interesting phenomena, namely a subgap energy state localized near the interface. This two dimensional interface considered to be the Fu-Kane superconductor and modeled by the Dirac like relativistic equation

$$\mathcal{H} = -i\hbar v_F(\sigma_x \partial_y - \tau_z \sigma_y \partial_x) + \tau_z \mu + \tau_y \sigma_y \Delta \quad (4.1)$$

is good up to some renormalization of the constants,  $v_F$ ,  $\mu$ ,  $\Delta$  as found in the previous chapter. This model was used in the first chapter to illustrate the existence of Majorana bound states localized where the effective mass term,  $\Delta$ , changes sign ( $\Delta \rightarrow -\Delta$ ) as in a Josephson  $\pi$  junction superconductor. This Majorana mode has a linear dispersion,  $E \propto \pm k$ . In this chapter we explore this  $\pi$  junction further, in particular for  $\mu \neq 0$ , where we find an energy dispersion that is flat and follows as  $E \propto k^N$ , where  $N$  scales with  $\mu$ . An extension of the the  $\pi$  junction is a periodic  $\pi$  junction where alternating  $(\dots -\Delta, \Delta, -\Delta, \Delta \dots)$  stripes of superconductors are placed in one direction. We find that this system also hosts the flat dispersion. We also find that the dispersion has “wiggles” when the spectrum is really closely analyzed.

### 4.1 Introduction

Moving at “the speed of light”,  $v_F$ , massless Dirac electrons on the surface of a three-dimensional  $Z_2$  topological insulator (TI) can not be localized by scattering from nonmagnetic impurities [7, 9], nor can they be easily confined by electrostatic potentials due to Klein tunneling [74]. Proximity coupling to ferromagnetic or superconducting order can however